Aguilar-Garcia et al. EURASIP Journal on Wireless Communications and Networking (2015) 2015:219
DOI 10.1186/s13638-015-0444-9

EURASIP Journal on Wireless Communications and Networking
a SpringerOpen Journal

RESEARCH Open Access

Enhancing RFID indoor localization with cellular technologies

A. Aguilar-Garcia[1*], S. Fortes[1], E. Colin[2] and R. Barco[1]

Abstract

Indoor localization, this means solutions providing the position of mobile objects/persons in indoor environments (e.g., hospitals, malls, etc.), is one of the most cutting-edge services with growing demand in smart applications such as robotics for care, pedestrian navigations, etc. With the objective of providing indoor localization, this paper presents the experimental analysis of simultaneous radio frequency measurements from two different radio frequency systems: Ultra High Frequency Radio Frequency IDentification (UHF RFID) and macrocellular networks. Extensively deployed cellular technologies (Global System for Mobile communications (GSM) and Universal Mobile Telecommunications System (UMTS)) are here evaluated with the purpose of enhancing pre-existent RFID-based localization systems at reduced costs. Temporal and statistical analysis of the measurements gathered from each technology is performed, and its applicability for localization is assessed. Based on this analysis, a RFID localization mechanism that is able to integrate macrocellular technologies information is proposed, showing improved results in terms of accuracy.

Keywords: UHF RFID; Cellular technology; Heterogeneous indoor localization; Fingerprint

1 Introduction

Several radio frequency-based systems have been proposed for providing indoor localization such as Ultra Wide Band (UWB), which presents location errors of few centimeters or Radio Frequency IDentification (RFID), which is in the range of few meters. However, accurate indoor positioning systems still present high costs in terms of hardware price, deployment expenditures, computational cost, and complexity, especially for very accurate solutions, such as UWB. In parallel, a wide variety of wireless communication networks coexist simultaneously with human beings. The results are the so-called Heterogeneous Networks (HetNets) where several wireless technologies surround daily life to create massive communication layers at different frequencies. These infrastructures provide a cloud of parallel information that could be, not only used for communication purposes, but also for enhancing accuracy and robustness of several a priori unrelated applications, such as indoor localization.

In this way, mechanisms for opportunistic radio positioning based on multiple techniques (e.g., wireless local area network (WLAN) together with Global System for Mobile communications (GSM), etc.) have been devised as promising solutions [1]. That integration of multiple technologies could lead to the required levels of accuracy at reduced costs. Macrocellular deployments for mobile communications are one of the most widely extended radio frequency (RF) technologies. However, up to our knowledge, its combination with RFID-based localization systems has not been previously envisaged in the literature. Therefore, this paper proposes and analyses the combination of a robust and reliable indoor positioning system such as RFID-based indoor positioning systems with another low-cost radio frequency solution in order to improve the accuracy of the indoor location-based services (LBS). Cellular technologies are selected in order to take advantages of the already deployed macrocellular networks.

A challenge for this solution is the lack of previous measurement campaigns including both cellular and RFID technologies, as well as defining systems for indoor localization able to integrate these two technologies. Therefore, this paper presents two main contributions.

* Correspondence: aag@ic.uma.es
[1]Departamento de Ingeniería de Comunicaciones, Universidad de Málaga, Andalucía Tech, Campus de Teatinos s/n, 29071 Málaga, Spain
Full list of author information is available at the end of the article

Firstly, the results of a radio frequency measurement campaign analyzing both RFID and cellular signals are presented and evaluated to determine whether there could be an improvement in indoor position calculation with the integration of cellular information into RFID-based localization systems. Secondly, a technique for integrating cellular technology information into indoor RFID-based localization systems is defined in order to improve the indoor location accuracy. Finally, the real field measurements are used to evaluate the capabilities of the proposed integrated localization system in comparison with pure RFID options.

The structure of this paper is as follows: the "State of the art" section details the state of the art of indoor localization technologies, focusing on wireless heterogeneous techniques. The "Technology general characteristics" section introduces an overview of theoretical propagation models for RFID and cellular networks. The "Localization techniques" section describes wireless indoor positioning techniques. The "Evaluation set-up" section presents the measurement equipment setup and the test-bed scenario where the experiments have been performed. The "Signal assessment" section details the gathered data and the assessment of the measurement campaign. The "Localization assessment" section evaluates the opportunistic capabilities of the proposed concept. Finally, the "Conclusions" section includes the conclusions and perspectives of this work.

2 State of the art

Indoor positioning and navigation is a field where the large diversity of application environments leads to a large diversity of solutions. A summary of the main positioning technologies, techniques, and their performances for typical applications are detailed in [2]. For these applications, several performance criteria can be defined, such as robustness, responsiveness, consumption, size, scalability, compatibility with human beings, accuracy, or precision.

Regarding camera-based systems, their high-security and confidentiality issues make them less accepted. Submetric radio frequency solutions as UWB, tactile and polar systems, or pseudolites use very expensive hardware while Infrared, sound, or HF RFID cover small areas and need numerous beacons or tags to be scalable.

Other radio frequency-based techniques are also widely used, but they do not provide enough accuracy for navigation positioning in indoor scenarios. In such techniques, metrics as received signal power (RSSI), angle of arrival (AoA) or time of flight (ToF) may not be directly related to distance or relative position between emitter and receiver. This is due to multipath and fading phenomena that can be dominating in indoor environments. Therefore, position estimation suffers from this initial uncertainty and sophisticated positioning algorithms, and filtering are needed to compensate these drawbacks.

In this respect, UHF RFID systems with active tags are not expensive, have an operating range of several tens of meters, and are easy to deploy, which comply with the application requirements for pedestrian navigation excepting for the accuracy. Indeed, their performance as commonly used is usually few meters [3]. Literature presented several passive UHF systems [4–6] to locate passive tags. They are used when covering small areas typically (3 m × 3 m), and their accuracy is in a range from 30 cm to 2 m, depending mainly on the tags density (from few tens to more than one hundred). They need at least 4 readers for this area (4 readers/10 m^2). The scalability of such a system remains a drawback, for example, to cover an entire floor of a public building of some hundreds square meters, a few hundreds of readers must be deployed.

The use of macrocell signal for outdoor localization has been previously assessed in studies like [7]. In outdoor scenarios, the signal coming from macrocell base station can be processed in order to obtain just a rough estimation of a mobile terminal position (hundreds of meters). Only particular indoor cellular deployments (such as small cells, low powered base station that can be installed indoors) have been analyzed [8]. In this field, the works [9, 10] presented a fingerprint technique based in the mapping and use of radio signals from femtocells (a particular type of small cells) for localization of mobile terminals in indoor environments (few meters). However, such indoor cellular deployments are still not widely implemented and costly.

The proposed option of combining UHF RFID tags with macrocell technology measurements could successfully provide the level of accuracy required in RFID-based localization systems for pedestrian navigation in buildings. More precisely, it will focus on indoor navigation in a floor of a building such as hospitals, universities, city halls, etc.

In this respect, the first works integrating diverse radio frequency technologies (not including RFID + macrocell, which has not previously considered) for indoor localization were presented a few years ago [1, 11]. The main purpose of combining different technologies is to increase the accuracy [12], or the density of the devices to be localized [13], or to overcome the continuity indoor/outdoor challenge [14], where these systems need to handle heterogeneous devices [15] and vertical handovers [1]. European Project WHERE2 [16] presented results of real-life experiments based on ZigBee and orthogonal frequency division multiplexing (OFDM) devices (emulating a multistandard terminal moving in typical indoor environments), with measurements using

Received Signal Strength Indicator (RSSI) and round-trip delay (RTD). A comparison between non-cooperative and cooperative positioning was done, and several positioning algorithms were tested in both cases. In reference [1], algorithms with realistic heterogeneous wireless networks, including GSM, Digital Video Broadcasting (DVB), frequency modulation (FM), and WLAN, were evaluated with measurements of RSSI. This paper proposed two cooperative positioning algorithms: Direct Multi-Radio Fusion (DMRF) reorganizes the information in a transformed space, and a Cooperative Eigen-Radio Positioning (CERP) uses the spatial discrimination property. Nevertheless, none of the previous works analyzed the promising approach of combining RFID and macrocell signal processing as a low-cost solution. In fact, up to our knowledge, there has not been any deep study in the field of combining UHF RFID with macrocellular signals. This is a suitable option for enhancing precision for pedestrian navigation in buildings with a highly reduced implementation costs in comparison with previous solutions. Such novel approach is presented in this work. Additionally, the proposed system would be only based on general commercialized hardware and software. This would include certain limitations in terms of the detail of the signal information (information about neighboring cells, SINR, etc.) available for the localization procedures. However, it is considered essential in order to facilitate the adoption of the system in operational deployments and common applications.

3 Technology general characteristics

In this section, the analyzed technologies are summarily described in based of their general characteristics and theoretical models in indoor scenarios.

3.1 RFID

For the RFID technology, there are two different types of systems: inductive and radiative, operating in a large range of frequencies, from 125 kHz to 5.8 GHz (Fig. 1), but most applications use LF, HF, and UHF bands.

Communication ranges of UHF systems are a few meters and up to 15 m in free space conditions. In order to achieve longer ranges beyond 15 m, transponders need a battery to provide power supply to the chip.

The power received for a line of sight (LoS) and multiple single reflections environment can be modeled as [17]:

$$\mathrm{RSSI}(d) = \left(\frac{\lambda}{4\pi d}\right)^2 \left|1 + \sum_{n=1}^{N} \Gamma_n \frac{d}{d_n} e^{-j(d_n - d)}\right|^2 \quad (1)$$

where λ is the wavelength, d the length of the direct ray path, Γ_n the reflection coefficient of the n-th reflecting object, d_n the length of the n-th reflected ray path, and N the total number of reflections.

The estimation of the multiple reflections in the scenario requires an accurate description of the environment. In practice, the most commonly used channel model for indoor scenarios is the log-normal shadowing model [18]. It allows to predict the path loss by a statistical analysis of measurements in a given physical surrounding:

$$\mathrm{PL}(d) = \mathrm{PL}(d_0) + 10\eta \cdot \log_{10} \frac{d}{d_0} + X_\sigma \quad (2)$$

where $\mathrm{PL}(d_0)$ is the path loss for a reference distance d_0, η is the path loss exponent, and X_σ is a Gaussian random variable with zero mean and a standard deviation σ.

3.2 Cellular technology

GSM is a standard that describes protocols for second generation (2G) mobile cellular networks. GSM systems usually work in the 900/1800 MHz band, whereas in the third generation (3G), Universal Mobile Telecommunications System (UMTS) is located at the 900/2100 MHz band (in Europe). Furthermore, there is also an important difference in terms of radio propagation: the carrier spacing is 200 kHz in GSM, whereas it is increased to

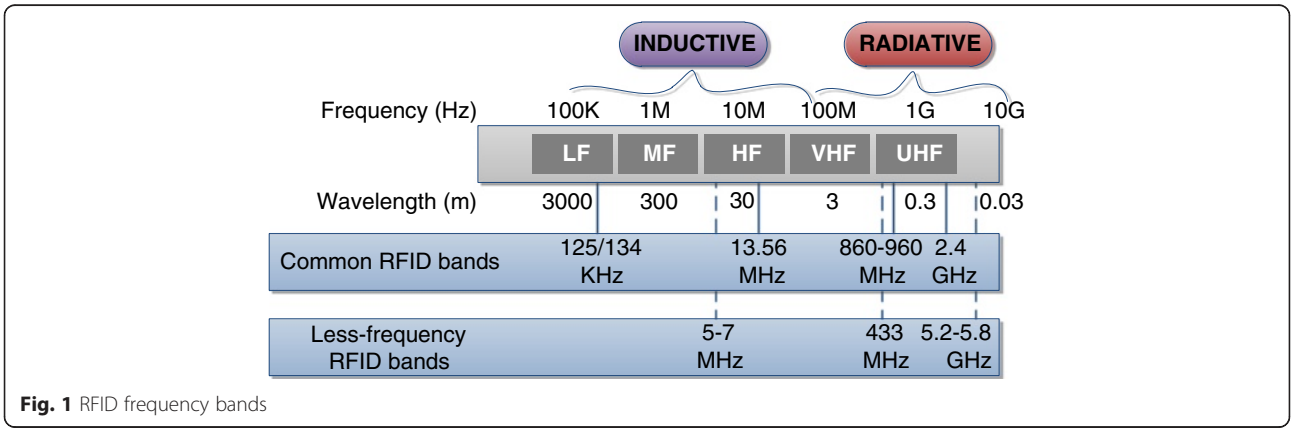

Fig. 1 RFID frequency bands

5 MHz in UMTS. For this reason, UMTS system is more vulnerable to frequency selective fading than GSM systems. Particularly, the wireless wave will be diffracted, scattered, and absorbed by the terrain, trees, building, vehicles, people, etc. that encompasses the propagation environment as it traverses the path from a transmitter to a receiver. The presence of obstacles along the path might cause the signal to experience higher attenuation than it would suffer under free space conditions.

Both GSM and UMTS technologies are widely implemented all over the world. Even if GSM is a legacy technology in terms of telecommunications, it is by far the most extended technology in terms of coverage and redundancy of macrocell stations, where also the lower transmission frequencies allow a better reception in the indoor scenario object of this study.

In order to obtain a glance of the cellular signal channel characteristics at the considered scenarios, COST231-Hata model [19] which is valid from 150 MHz to 2 GHz and WINNER II model [20] which is valid from 2 to 6 GHz can be adopted as two of the most widely propagational models for cellular communication studies.

COST231-Hata model defines the path loss in different urban and suburban areas as well as in in-building penetration. This model uses a LoS path loss with an indoor component:

$$\mathrm{PL}(d) = 32.4 + 20 log f_{\mathrm{GHz}} + 20 log(d_{\mathrm{out}} + d_{\mathrm{in}}) + \mathrm{PL}_{\mathrm{in}} \tag{3}$$

where f_{GHz} is the frequency in GHz, d_{out} is the outdoor path, d_{in} is the indoor path, and $\mathrm{PL}_{\mathrm{in}}$ is defined as:

$$\mathrm{PL}_{\mathrm{in}} = \mathrm{PL}_e + \mathrm{PL}_{\mathrm{ge}}(1 - sin\theta)^2 + max(\Gamma_1, \Gamma_2) \tag{4}$$

where PL_e is the normal incidence first wall penetration, $\mathrm{PL}_{\mathrm{g}e}(1 - sin\theta)^2$ is the added loss due to angle of incidence θ which is usually measured over an average of empirical values of incidence, and $\max(\Gamma_1, \Gamma_2)$ estimates loss within the building.

WINNER II model defines different scenarios and their applicable path loss characteristics. For the case of macrocellular signal reaching in indoor environments, the correspondent model is outdoor-indoor C4. The expression for this model path loss is:

$$\mathrm{PL}(d) = \mathrm{PL}_{C2}(d_{\mathrm{out}} + d_{\mathrm{in}}) + 17.4 + 0.5 d_{\mathrm{in}} - 0.8 h_{\mathrm{MS}} \tag{5}$$

where d_{out} is the distance between the macrocellular station and the external wall of the indoor scenario, d_{in} is the distance between the wall and the receiver indoors, PL_{C2} represents the path loss for the model for urban macrocell outdoors, and h_{MS} is the height of the mobile station. For this model, the impact of d_{in} in the factor PL_{C2} $(d_{\mathrm{out}} + d_{\mathrm{in}})$ becomes usually negligible for the normal distance of dozens/hundreds of meters between the indoor building and the macrocell base station. This makes the evolution of the path loss in the indoor scenario mainly influenced by the term $0.5 d_{\mathrm{in}}$.

Additionally, the impact of the shadow fading can be also modeled for an indoor scenario as a log-normal distribution with standard deviation of 8 dB. Finally, fast fading can be modeled as Rayleigh (in non-line of sight) and Ricean (in line of sight situations) distributions. However, fast-fading effects are mostly eliminated in the measurements provided by common-monitored tools due to the integration of the signal during the measurement periods (lasting commonly 1 s). This makes the shadowing the main component for the difference of received power between positions of the scenario. Still, in order to categorize the characteristics of each location, shadowing effects cannot be calculated without very complex computations, and an extremely detailed knowledge of the scenario is required. Furthermore, the path followed by the signal from the macrocellular base station to the terminal shall be known.

4 Localization techniques

To determine the possible improvement achievable by the combination of RFID and cellular technologies, different baseline single-technology localization solutions are defined. Then, a method for their integration is proposed. These mechanisms would be specifically tuned and evaluated on the measurement campaign data in the "Localization assessment" section.

4.1 General scheme

Fingerprinting-based techniques are selected to provide indoor localization, being a widely applied scheme for localization in these environments [21]. These techniques are defined by two main phases, *calibration* (offline) and *localization* (online):

- Calibration phase: This stage is performed prior to the provision of the localization service. Here, RSSI values and transmitter identifiers (the transmitted identification of a specific cell or tag) are collected at known locations of the scenario. This information is then stored in a database as calibration maps of the environment.
- Localization phase: It consists in the online provision of the localization service. Here, the set of measurements received in real time by the localized platform are used to estimate its position by means of comparing it to the stored calibration map.

4.2 Baseline localization phase algorithms

For the case where a unique technology (RFID or cellular) is used for localization, there are multiple mechanisms available for the localization phase [21]. Here, the identification of the current position can be based in two different *comparable variables*:

- Prx: the received power level from a set of transmitters (cell and/or tag),
- IDSrx: the particular set of "visible" transmitter identifiers (those that are received with at least a certain minimum power) at the particular location.

For both factors, the different baseline algorithms to be used in the system evaluation are presented in the following subsections. These follow the scheme presented in Fig. 2, which distinguish three steps to weight the candidates from the calibration phase points, intersect those candidates, and estimate a specific location.

4.2.1 Candidate positions weighting

Each calibration point (also denominated as *candidates*) $\gamma_f = (x_f, y_f, z_f)$ of the set of locations measured in the fingerprinting set $\mathbf{\Gamma}_f$ is weighted in relation to its radio similarity with the radio values currently gathered in the unknown position of the localized platform $\gamma_{\text{curr}} = (x, y, z)$. Three different approaches are described for defining the weight given to each calibration point, $w(\gamma_f, \gamma_{\text{curr}})$.

- Number of matches: the candidate positions are ranked by the number of coincidences with the current values: e.g., the number of tags received with the same average power level than the current one. $w(\gamma_f, \gamma_{\text{curr}})$ is calculated as the sum of all matches divided by the total number of possible matches. For example, if only RFID signal is used and there are 30 tags in the scenario, the number of possible matches with that technology is 30. Depending on the received power values or the identifiers, match definition will vary. On the one hand, if the coincidence is based on received power level Prx_i received from a transceiver i, a match is defined as:

$$\text{match}\left(\gamma_f, \gamma_{\text{curr}}\right)_{\text{Prx}_i} = \begin{cases} 1 & \text{if} \mu_{\text{Prx}_i}\left(\gamma_{\text{curr}}\right) \in \left[\mu_{\text{Prx}_i}\left(\gamma_f\right) - \Delta\text{Prx}, \mu_{\text{Prx}_i}\left(\gamma_f\right) + \Delta\text{Prx}\right], \\ 0 & \text{otherwise} \end{cases} \tag{6}$$

where $\mu_{\text{Prx}_i}(\gamma_f)$ is the mean received power from the transmitter i at the calibration point γ_f. $\mu_{\text{Prx}_i}(\gamma_{\text{curr}})$ is the mean power measured during the *acquisition time* in the localization phase at the current position γ_{curr} (to be estimated). The acquisition time is the period of monitoring of the network used by the mobile localized platform to obtain a specific radio measurement/value. As it will be further described in the following sections, this may be obtained from a unique measured value or it may be the result of average of multiple samples. ΔPrx is an established error margin: in the evaluation section, the

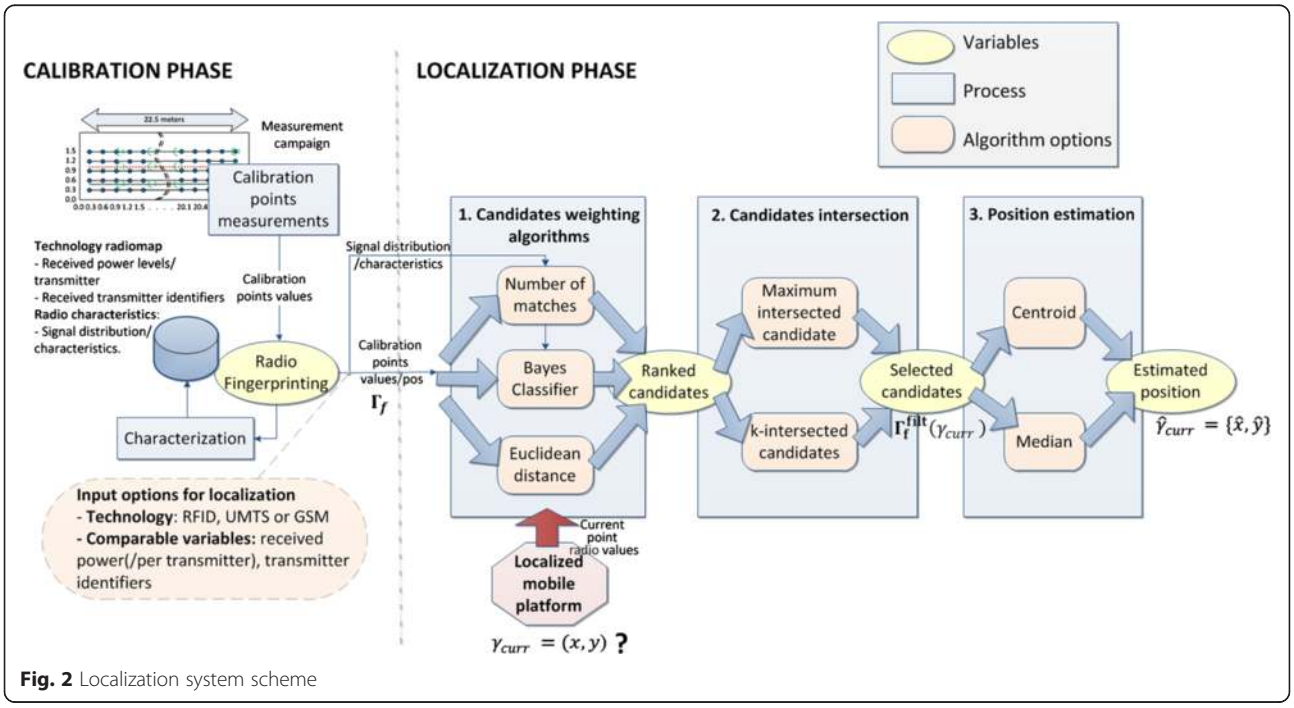

Fig. 2 Localization system scheme

algorithm will be tested with different values of this margin.
On the other hand, if the similarity is measured in based of the received identifiers, a match is defined as:

$$\text{match}\left(\gamma_f,\ \gamma_{\text{curr}}\right)_{Id} = \begin{cases} 1 & \text{if } \text{Id}(\gamma_{\text{curr}}) \cap \text{Id}\left(\gamma_f\right) \neq 0 \\ 0 & \text{otherwise} \end{cases}, \quad (7)$$

where $\text{Id}(\gamma_f)$ is the set of received identifiers at the calibration point γ_f and $\text{Id}(\gamma_{\text{curr}})$ is the set of identifiers received at the current position γ_{curr} during the acquisition time in the location phase. The expressions mean that in case both sets shared common identifiers, the match is considered affirmative.

- Bayes Classifier: In this method, the weight of the candidates is defined as the posterior probability of being in the calibration point given the current mean power values received $\hat{p}\left(\gamma_{\text{curr}} = \gamma_f | \mu_{\text{Prx}}(\gamma_{\text{curr}})\right)$. This is calculated by means of a naive Bayes classifier:

$$\hat{p}\left(\gamma_{\text{curr}} = \gamma_f | \mu_{\text{Prx}}(\gamma_{\text{curr}})\right) = \frac{\hat{p}(\gamma_f) \prod_{\forall i \in I} \hat{p}\left(\mu_{\text{Prx}_i}(\gamma_{\text{curr}}) | \gamma_f\right)}{\hat{p}\left(\mu_{\text{Prx}}(\gamma_{\text{curr}})\right)}, \quad (8)$$

where

- $\hat{p}\left(\mu_{\text{Prx}_i}(\gamma_{\text{curr}}) | \gamma_f\right)$ is the *conditional probability* of receiving $\mu_{\text{Prx}_i}(\gamma_{\text{curr}})$ in the candidate position γ_f from the transmitter $i \in I$ (I being the set of considered transmitters).
- $\hat{p}\left(\gamma_f\right)$ is the estimated *prior probability* of being in each candidate position. For the assessment of the system, a no-memory mechanism is assumed, and therefore, each candidate point would be considered equally probable.
- $\hat{p}\left(\mu_{\text{Prx}}(\gamma_{\text{curr}})\right)$ is the likelihood of the evidence (the current mean power values). For the ranking, $\hat{p}\left(\boldsymbol{\mu}_{\mathbf{Prx}}(\gamma_{\text{curr}})\right)$ can be discarded as it is the same for all candidates.

Therefore, the expression for weighting each candidate can be simplified as:

$$p\left(\gamma_{\text{curr}} = \gamma_f | \mu_{\text{Prx}}(\gamma_{\text{curr}})\right) \propto \prod_{\forall i \in I} p\left(\mu_{\text{Prx}_i}(\gamma_{\text{curr}}) | \gamma_f\right), \quad (9)$$

where $\hat{p}(\mu_{\text{Prx}_i} | \gamma_f)$ is the probability density function (PDF) of the conditional probabilities for each candidate position, γ_f, and tag i. This PDF is estimated assuming a normal distribution (a common approach for modeling the received power) with mean and standard deviation in base of the samples gathered in the calibration phase (as represented by the module characterization in Fig. 2). Then, Laplace smoothing [22] is applied to the PDF to avoid giving zero probability to current RSS values, as this might eliminate possible good candidates just for the incorrect reception of one tag. The PDF is then used to calculate the conditional probability of the current mean received power.

- Euclidean distance: this method is well known in the literature [23]. Firstly, for each calibration point, the vector of the mean received power from all the transmitters is defined as $\mu_{\text{Prx}}(\gamma_{\text{curr}}) = \{\mu_{\text{Prx}_1}(\gamma_f), \mu_{\text{Prx}_2}(\gamma_f) \ldots\}$. Then, its weight is calculated as the distance between such vector and the one formed from the current received power levels $\mu_{\text{Prx}}(\gamma_{\text{curr}})$ gathered by the localized platform:

$$w(\gamma_f, \gamma_{\text{curr}}) = d\left(\mu_{\text{Prx}}(\gamma_f), \mu_{\text{Prx}}(\gamma_{\text{curr}})\right)$$

4.2.2 Candidates intersection

Whereas the previous step provided a ranking of the candidates similarities, this step serves to filter the total number of considered positions from the original set of calibration points $\boldsymbol{\Gamma}_{\mathbf{f}}$ to a reduced one $\boldsymbol{\Gamma}_{\mathbf{f}}^{\mathbf{filt}} \subseteq \boldsymbol{\Gamma}_{\mathbf{f}}$. Two different techniques are tested for this step:

- Maximum intersected candidate (mic): the system selects uniquely the candidate or candidates (if more than one shares the same maximum weight) with the highest ranking achieved by the calibration points, this means: $\Gamma_{\text{f}}^{\text{filt}}(\gamma_{\text{curr}})_{\text{mic}} = \left\{\gamma_f,\ \forall \gamma_f \epsilon \Gamma_{\text{f}} \middle| w\left(\gamma_f,\ \gamma_{\text{curr}}\right) = \max\left(w(\Gamma_{\text{f}},\ \gamma_{\text{curr}})\right)\right\}$.
- k-intersected candidates (kic): the filtered candidates $\boldsymbol{\Gamma}_{\mathbf{f}}^{\mathbf{filt}}(\gamma_{\text{curr}})_{\text{kic}}$ are those with the k highest weights; this means those with weights equal to the maximum weight achieved max ($w(\Gamma_{\text{f}}, \gamma_{\text{curr}})$) and the subsequent k lower levels. This implies that the number of candidates in the filtered set is equal or higher than k : $|\Gamma_{\text{f}}^{\text{filt}}(\gamma_{\text{curr}})_{\text{kic}}| \geq k$.

4.2.3 Position estimation

The filtered candidates from the previous stage are then used to estimate the current position of the mobile localized platform. For these, two main mechanisms are analyzed:

- Centroid (geometric center): the estimated position $\hat{\gamma}_{\text{curr}} = \{\hat{x}, \hat{y}, \hat{z}\}$ is calculated as the geometric center of the filtered candidates. Assuming a fixed

height, the estimated coordinates of the point will be calculated as:

$$\hat{x} = \frac{1}{\left|\Gamma_{\mathrm{f}}^{\mathrm{filt}}\left(\gamma_{\mathrm{curr}}\right)\right|}\sum_{x_f \in X_f^{\mathrm{filt}}} x_f \quad ; \qquad \hat{y} = \frac{1}{\left|\Gamma_{\mathrm{f}}^{\mathrm{filt}}\left(\gamma_{\mathrm{curr}}\right)\right|}\sum_{y_f \in Y_f^{f\mathrm{filt}}} y_f \tag{10}$$

$\left|\Gamma_{\mathrm{f}}^{\mathrm{filt}}\left(\gamma_{\mathrm{curr}}\right)\right|$ where $\bar{x}$ and $\bar{y}$ are the coordinates of the calculated centroid, $\left|\Gamma_{\mathrm{f}}^{\mathrm{filt}}\left(\gamma_{\mathrm{curr}}\right)\right|$ is the number of filtered positions-candidates, and $\left(x_f \in X_f^{\mathrm{filt}}, \cdot y_f \in Y_f^{\mathrm{filt}}\right)$ represents the coordinates of that candidate positions.

- Median: In this case, the position is estimated by assigning it the median of each coordinate of the filtered candidates.

4.3 Integration of cellular technology into RFID-based localization system

As an example of the possibilities of combination of the data coming from both technologies, a new scheme for enhanced indoor localization based on these heterogeneous technologies is proposed in Fig. 3. Here, in order to assess the advantages of having both cellular and RFID signal in the presented system/scenario, a baseline approach for the integration of both systems is proposed.

This consists in the data fusion of the RFID-based generated candidates with the ones obtained from the cellular system. Even if other approaches are possible, this work integrates results from the independent output of both RFID and cellular systems. These solutions allow a clear comparison of the gain of the integrated system as well as facilitates its integration in already existing services. With this objective, the proposed mechanism defines two main steps:

1. Cellular geometric discrimination: the RFID filtered candidates per position $\Gamma_{\mathrm{f,\,RFID}}^{\mathrm{filt}}$ are discriminated by the cellular filtered candidates $\Gamma_{\mathrm{f,\,CELLULAR}}^{\mathrm{filt}}$ as follows: an area of 1 m^2 (maximum distance between two adjacent points in the cellular fingerprint matrix) is created for each cellular candidate position in order to evaluate if any of the RFID candidates are located inside this area. In this case, the RFID candidate is selected, whereas any other candidate outside those areas is discarded. In case none of $\Gamma_{\mathrm{f,\,RFID}}^{\mathrm{filt}}$ candidates match, none of them is discarded.
2. Opportunistic localization: once the candidates have been selected based on the combined cellular and RFID information, the estimated position is calculated by centroid or median metrics.

5 Evaluation setup

Once the general characteristics of the technologies and localization mechanisms have been detailed; a description of the proposed architecture and the measurement campaign, as well as the equipment used to transmit and receive the wireless signals, are specified in this section.

While providing pedestrian localization in buildings, navigation is done through large halls and corridors. In this case, unlike passive RFID, our solution with active technology can cope with the reading range requirements in large areas. In this work, we focus on a corridor environment which is a more critical environment than halls in terms of multipath propagation.

5.1 Proposed architecture

A specific architecture for the implementation of the integrated RFID and cellular localization system is

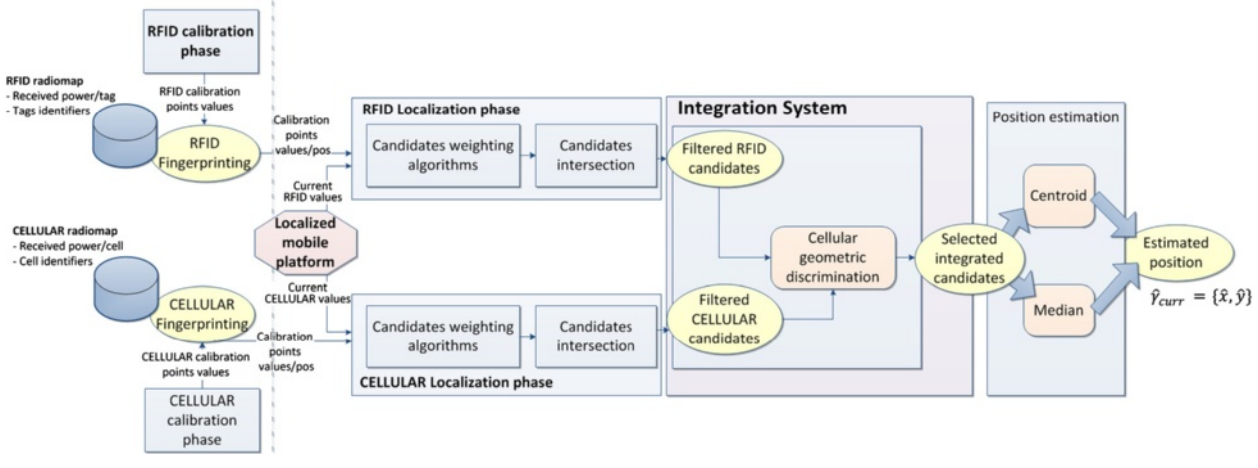

Fig. 3 Integration of cellular technology into RFID-based localization system scheme

proposed in Fig. 4. Here, a cloud-computing scheme is assumed, where most part of the localization algorithm computation is performed externally by a remote entity. This is a widely extended approach in localization systems in order to reduce the computational and storage costs for the *mobile localized platform* (the mobile object which position is calculated), at the cost of increasing the requirement of maintaining a continuous communication with the external entity. In this scheme, the information transmitted to the external entity can consist just in the received power levels and source identifier.

5.2 Simulations

As support for the real-world characterization of the signal, their behavior is emulated by means of simulations for each technology. The selected indoor scenario consists on a corridor 22.5 m long × 2 m width (same scenario as it will be described in the measurement campaign):

- RFID: A tag is emulated on the left wall of the corridor in the position (0,1). For simplicity, the radio propagation model predicts the signal received in line of sight and multipath component formed predominately by a single reflected wave. The power transmission of the tag was set to −30 dBm.
- UMTS and GSM: Three tri-sectorized macrocells have been deployed into a large scenario to cover the designed corridor for both technologies. They are placed 1 km far from the corridor.

The results of these simulations are compared with the results obtained for the real-world prototype presented in the following section.

5.3 Real-world prototype

5.3.1 Scenario

For indoor location in a building, three main types of environments could be found: halls, corridors, and offices. For offices and rooms, simple detection of presence in the room could be enough for many applications. However, accurate indoor positioning systems are specially required in corridors and halls with multiple doors. Such areas (e.g., hospital corridors surrounded by patient rooms) act as distributors to different locations making essential a precise position estimation of the localized platform. This is the reason why this paper has focused on measurements in corridors. This study has been carried out into a 4th floor indoor offices building (526 m2), along the corridor, which is 22.5 m long × 2 m width × 2.5 m height as it can be seen in Fig. 5.

5.3.2 RFID equipment

Thirty UHF RFID active tags were deployed on the walls of the corridor in order to ensure the lowest location error. They were placed at 1.40 m and 2.10 m height alternatively in both sides of the corridor while the distance between two tags was 1.5 m. Those heights respectively correspond to a doorknob and a standard door height. The layout and the position of the tags in the corridor are illustrated in Fig. 6.

Note that no tag has been placed on the ceiling because of the specific radiation pattern of the reader

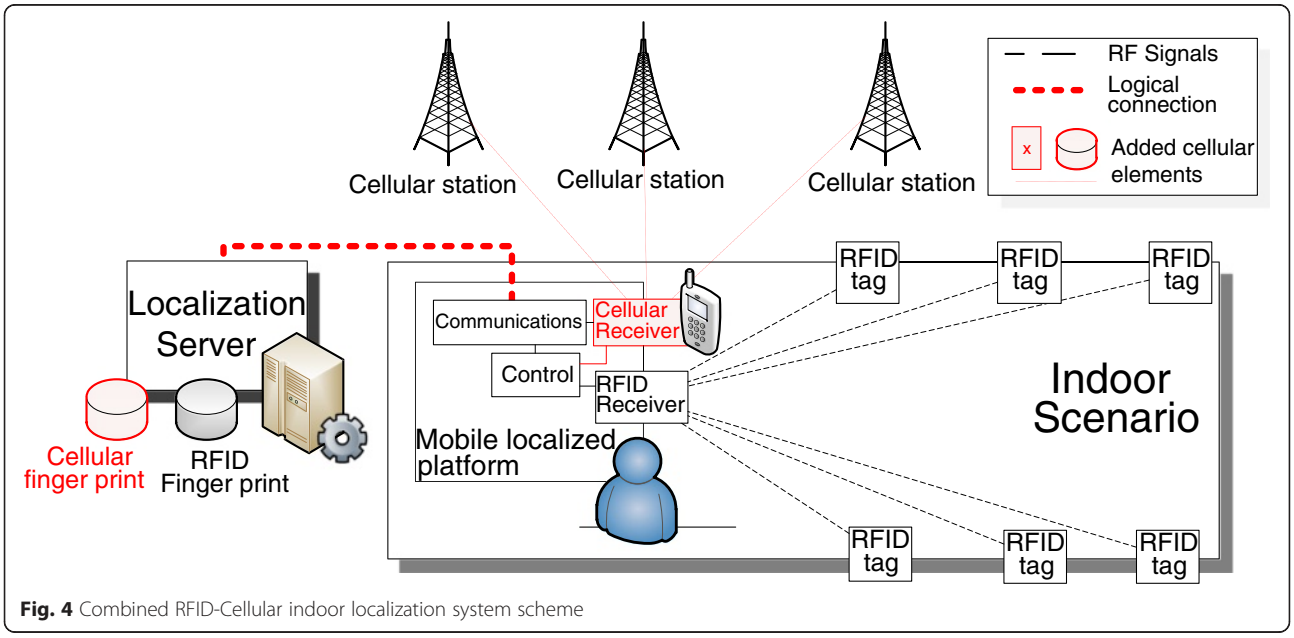

Fig. 4 Combined RFID-Cellular indoor localization system scheme

Fig. 5 Corridor, tags placement, and mobile-localized platform

antenna. A zero is in the axis of the dipole that is to say towards the ceiling and the floor.

These positioning devices use 433 MHz (ISO 18000–7) RFID technology. The reader model is "UTPDiff2" with two vertical dipole Rx/Tx antennas, and the active tags are the "Thinline" model both from Ela-Innovation [24]. Tags can be detected from as far as 40 m in an indoor environment.

5.3.3 Mobile communications equipment

For cellular network assessment, two smartphones were used in the experimental evaluation: Samsung Galaxy S3 and a Sony Ericsson Xperia X10 Mini E10i (as it will be later described, the former was used to measure UMTS technology and the later to measure GSM). They are widely extended commercial models running Android 4.2 and Android 2.1, respectively. Additionally, to measure and record the received power in those devices, a popular free Android application for cellular monitoring, G-MoN [25], was used. This app is a powerful tool for monitoring cellular and other wireless technologies as a drive test tool. It provides cellular network information such as RSS, cell ID, local area code (LAC), etc. At the same time, these data are stored in a local file. Note that RSS values are averaged at Layer 1 and 3 [26] of the terminal protocol stack minimizing the impact of fast fading in its values. Therefore, the app reported RSS reflects the path loss and shadowing characteristics of the signal.

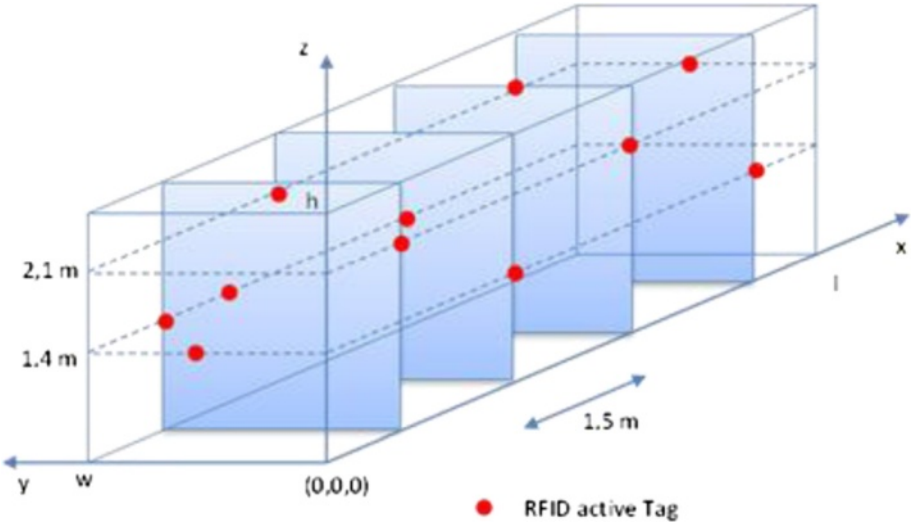

Fig. 6 Tags location in the corridor

5.3.4 Platform

The mobile phones and RFID reader were located on top of a trolley as Fig. 5 depicts. The measurements have been carried out for two different cellular technologies at the same time. The Samsungs smartphone was forced to be camped on a UMTS macrocell area whose frequency band was 2100 MHz. Likewise, the other smartphone was pushed to be connected to the GSM network at 900 MHz frequency band. This technology diversity (433, 900 and 2100 MHz) allows a complete study in indoor real scenario conditions in order to enhance localization systems as it will be analyzed in the next sections.

5.3.5 Measurable parameters

On the one hand, with the presented RFID equipment, the main parameters that can be measured per tag in a certain time slot are the following:

- Tag ID: numerical identifier of the tag being received by the reader (multiple tags can be simultaneously received).
- Received power (dBm) quantified with a resolution of 0.6 dBm from 118 for −44 dBm to 215 for −106 dBm.

On the other hand, for cellular signals, the main parameters that can be measured by common terminal apps are the following:

- CellID, the numerical identifier of the serving cell of the mobile terminal.
- Received power (dBm), quantified with a resolution of 1 dBm in the range (−115, 0) dBm.

6 Signal assessment

For the assessment of the RFID and cellular signals under study, several samples were collected for each technology along the corridor: three lines of measurements (called hereafter "left," "middle," "right") were performed along it with a distance of 50 cm from each other (see Fig. 5) where multiple samples have been gathered every meter for each position. This provides 63 positions (21 per line) in the whole corridor.

Both systems (RFID and cellular) acquire samples during 5 min per position. Regarding the RFID system, all tags are sampled every 5 s while the cellular signal (GSM and UMTS signals) were measured every second. In order to simplify the assessment, all measurements were taken with the same orientation (see Fig. 5). Notice that, assuming that the cellular terminals properly report the terminal orientation, the analysis of the signal and/or the calibration phase can be performed and stored for multiple orientations. Then, during the localization phase, data from training sets with different orientations would be selected and combined following common approaches for positioning.

These experiments were carried out in the morning of 3 days. During the assessment campaign, the corridor was empty (no furniture and no people walking along), and doors remained closed to avoid additional fading or extra scattering sources.

In order to analyze the characteristics of radio signals received from each technology and to assess their applicability for indoor location, the following statistics have been studied:

- Complete distribution: referring to the range and distribution of signal values in terms of the IDSrx and Prx. From the point of view of the Prx, this distribution is characterized by the mean $\mu_{\text{Prx}}^{\text{complete}}$ and standard deviation $\sigma_{\text{Prx}}^{\text{complete}}$ of all samples gathered in the assessment. From the perspective of the IDSrx (the number of distinct identifiers detected), the number of identifiers $N_{\text{IDSrx}}^{\text{complete}}$ is measured.
- Per position analysis: about the variability of the gathered signals received in each fixed position. It gives an idea of the stability of the signal and therefore the achievable accuracy of the localization system. For this perspective, different statistics have been defined:
  - $\sigma_{\text{Prx}}^{\text{static}}(x,y)$, $\mu_{\text{Prx}}^{\text{static}}(x,y)$—static standard deviation and mean of Prx (in dB): it measures the level and stability of the power measurements in a specific position (x, y):

$$\sigma_{\text{Prx}}^{\text{static}}(x,y) = \sqrt{\frac{1}{|M_{x,y}|}\sum\nolimits_{\forall m_i \in M_{x,y}} \left(m_i - \mu_{\text{Prx}}^{\text{static}}(x,y)\right)^2}, \tag{11}$$

    where $M_{x,\,y}$ is the set of $|M_{x,y}|$ received power samples m_i measured in the (x, y) position and $\mu_{\text{Prx}}^{\text{static}}(x,y)$ is the average of the $M_{x,\,y}$ samples.
  - $\sigma_{\text{Prx}}^{\text{adjacent}}(x,y)$—adjacent standard deviation of Prx (in dB): it is calculated as the deviation of the set of the received power values in one position and its adjacent points in the assessment set:

$$\sigma_{\text{Prx}}^{\text{adjacent}}(x,y,) = \sqrt{\frac{1}{|M_{x,y}^{\text{adj}}|}\sum\nolimits_{\forall m_i \in M_{x,y}^{\text{adj}}} \left(m_i - \mu_{\text{Prx}}^{\text{adjacent}}(x,y)\right)^2}, \tag{12}$$

    where $M_{x,y}^{\text{adj}} = \left\{M_{x,y} \cup M_{x+x0,y} \cup M_{x-x0,y} \cup M_{x-x0,y-y0} \ldots\right\}$ is the set of Prx measurements used in the assessment, being $\{(x + x0, y)\ldots\}$ as the adjacent positions in the calibration (variations in the z axis are not considered in our case due to the fixed height of the target platform). $\mu_{\text{Prx}}^{\text{adjacent}}(x,y)$ is the

mean of the $M_{x,y}^{\text{adj}}$ samples. This provides an assessment on the discernibility of a position in respect to its neighbors in terms of Prx.

- $N_{\text{IDSrx}}^{\text{static}}(x,y)$—static number of IDSrx: it refers to the *number* of serving cellular base stations or tags measured per point. For RFID, where the receiver is able to receive multiple transmitters, it is an indication of the amount of Prx sources of information available per point. If only a transmitter is received each time (as in cellular terminals where only the serving cell may be considered), this parameter provides an assessment of the stability of the serving transmitter reception in each position. Different cells can served the same point at different instant as results or similar level of power and time changing fading effects.
- $\sigma_{\text{IDSrx}}^{\text{adjacent}}(x,y)$—adjacent ratio of common IDSrx: it indicates the number of IDSrx different between one position and its adjacent ones. Such parameter measures the possibility of using the cellID to distinguish between positions.

As these statistics are computed for each position, their mean or median for all the calibration points of the scenario can be calculated, as it is presented in the "Applicability of the results" section, providing a numeric overview of the characteristics of the different technologies along the scenario.

In the following subsections, the features of the different signals are analyzed from the simulated scenario and the real prototype area described before.

6.1 RFID signal

6.1.1 Complete distribution

For the simulated signals, the probability distribution function (PDF) for a tag placed on coordinates (0,1) and per line of measurement are illustrated in Fig. 7. For the middle line, Fig. 7b, it presents a value of $\sigma_{\text{Prx}}^{\text{complete}} = 6\,dB$.

Regarding the real campaign, the probability distribution function at each line along the corridor for a random RFID tag is represented in Fig. 8, which has been constructed aggregating 1260 (21 positions × 60 samples/position) measurements per line. In this case, the average power $\mu_{\text{Prx}}^{\text{complete}}$ for this particular tag is around –60 dBm for all lines, but distribution is more symmetrical for the middle line, Fig. 8b. Here, the received power is between (–73, –43) dBm and a value of $\sigma_{\text{Prx}}^{\text{complete}} = 7.3$ dB, which is consistent with the simulated results. Given their positioning, all of the installed tags are received at some point of the scenario, making $N_{\text{Id}}^{\text{complete}}$ equal to 30.

Finally, comparing both figures, quite similar distributions are observed between the simulation results and the measurement campaign.

6.1.2 Per position analysis

Figure 9 shows the measurements gathered in the middle line of the corridor coming from two representative tags located at the beginning (a) and in the middle (b) of the corridor. Indeed, mean power per position along the corridor $\mu_{\text{Prx}}^{\text{static}}(x,y)$ is ranged from –45 to –75 dBm (green dots) for most positions, which complies with the path loss slope using the log-normal model in this corridor.

Prx deviation per position, $\sigma_{\text{Prx}}^{\text{static}}(x,y)$, is quite low. In average, along the corridor, the mean of the deviation values is less than 1 dB (blue line). Similar results are obtained for the rest of the 30 tags.

6.2 Cellular signal

6.2.1 Complete distribution

On the one hand, regarding the simulation results, Prx probability distribution functions are illustrated in Figs. 10 and 11. For the cellular case, Prx is considered independently of the serving cell (serving cell received power is used without examining its cellID). UMTS technology, presents a value of $\sigma_{\text{Prx}}^{\text{complete}} = 7.6\,\text{dB}$, showing a

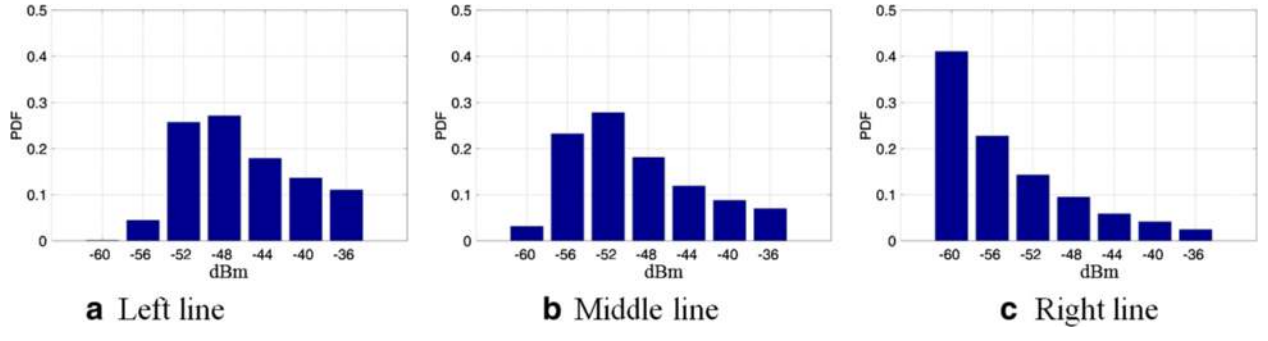

Fig. 7 RFID—Histograms (simulations) for the left (**a**), middle (**b**) and right (**c**) lines

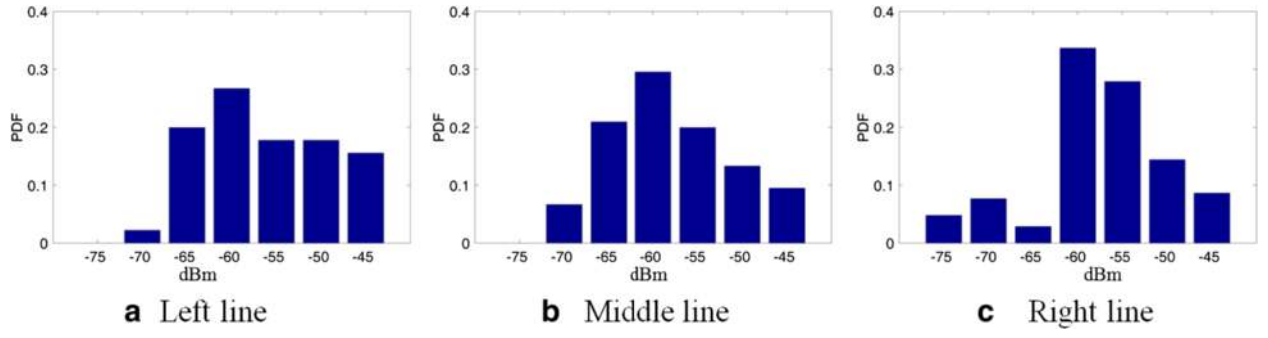

Fig. 8 RFID—Histograms for the left (**a**), middle (**b**) and right (**c**) lines

wide variability of the received power suggesting the presence of important shadowing effects in the corridor. Regarding GSM information, this has a value of $\sigma_{\text{Prx}}^{\text{complete}} = 11.2\,\text{dB}$, having a dominant power component in the three histograms which suggest the presence of a dominant direct line of sight between the macrocell and the corridor. In terms of variable range, both technologies cover around 40 dB from the minimum to the maximum measured value.

On the other hand, the results of the real prototype campaign are also described. Firstly, for the UMTS technology, the global statistical distribution of all measurements in the corridor is represented in Fig. 12, which has been calculated aggregating 6300 (21 positions × 300 samples/position) measurements per line. Here, it can be observed how the measurements are mainly in the range of (−104, −88) dBm in every line, showing the wide variability in the values of the received power along the corridor, with a value of $\sigma_{\text{Prx}}^{\text{complete}} = 4.13\,\text{dB}$ for the middle line. This could mean two different situations: either the received power suffers quick changes due to the fading or the signal is more or less stable around the same position but it changes a lot with the position. However, the dominant power component around −98 dBm suggests a stable signal in the corridor.

Secondly, for the GSM technology, Fig. 13 illustrates the same information. In this case, the average received power is higher than for UMTS. The range width, mainly between (−90, −75) dBm, provides similar values to UMTS, but the deviation is higher $\sigma_{\text{Prx}}^{\text{complete}} = 7.5\,\text{dB}$.

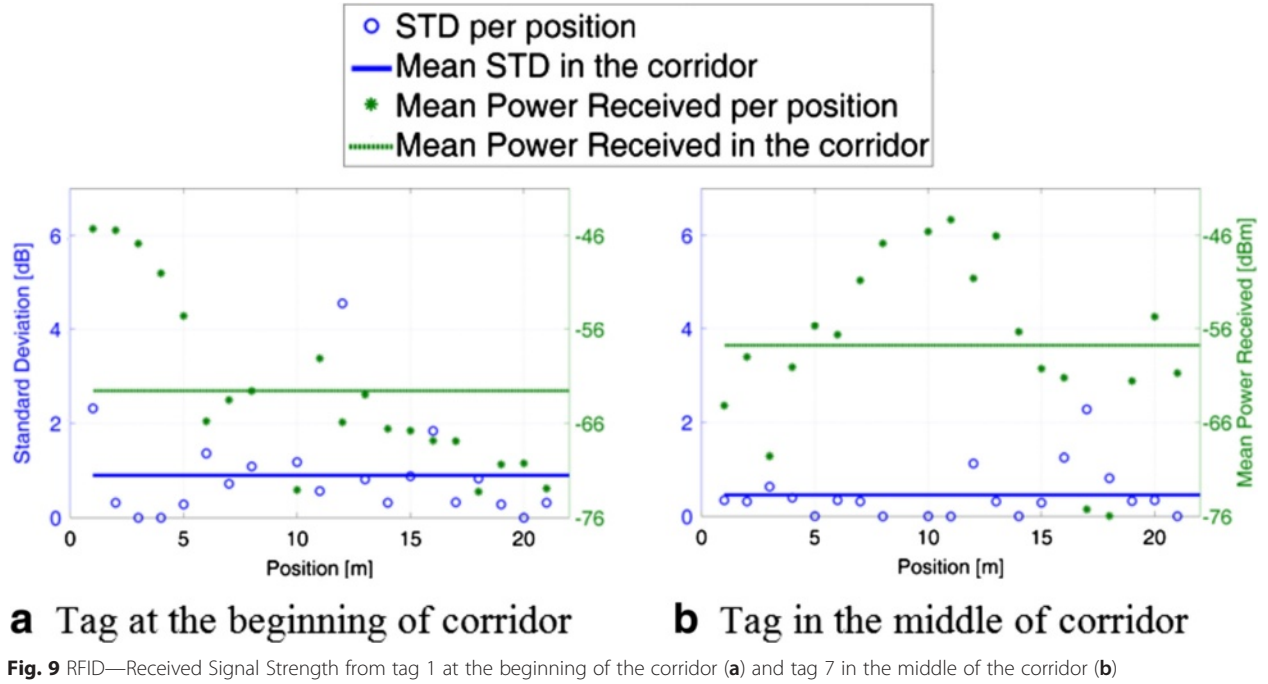

Fig. 9 RFID—Received Signal Strength from tag 1 at the beginning of the corridor (**a**) and tag 7 in the middle of the corridor (**b**)

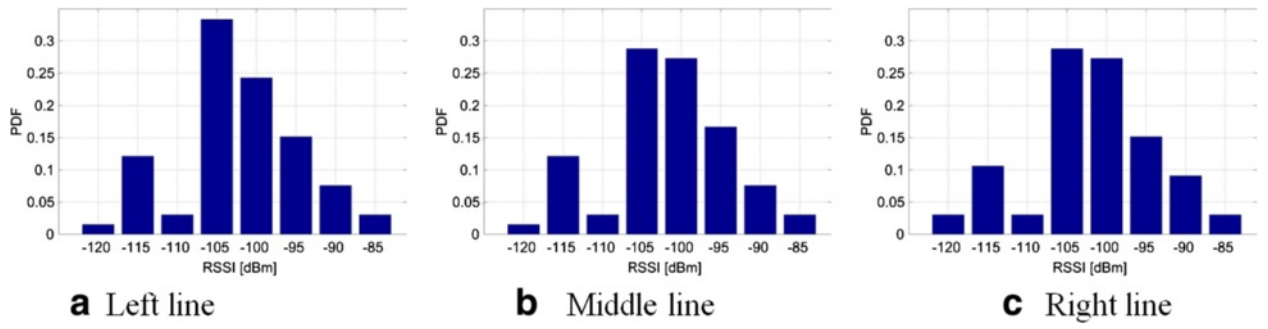

Fig. 10 UMTS—Histograms (simulations) for the left (**a**), middle (**b**) and right (**c**) lines

This is consistent with the GSM band being located in the lower frequencies (900 MHz) than UMTS (2100 MHz), which makes it less affected by attenuation and common obstacles in indoor environments. This would depend also on the location of the cellular base station, but in this case, and following common cellular telecommunications operators practices, both technologies share the same site, therefore, the same distance to the studied scenario. In these histograms, it is shown two main ranges of dominant power components, which could mean that two serving cells are received in the corridor.

The measurements show a narrower distribution than the simulated results due to the different shadowing conditions. However, the general relation between the characteristics of both technologies, with a higher deviation for GSM, is consistent with the simulated results.

6.2.2 Per position analysis

Furthermore, as analyzed for the previous RFID technology, one of the main characteristics in the use of radio signals for localization and/or monitoring purposes is the degree of stability of the signal for a specific position.

On the one hand, to analyze the signal stability from the point of view of the received power, its standard deviation and mean are calculated for all the measurements gathered in each different position. For that purpose, G-MoN app automatically sniffs cellular signals and provides cellular information each second.

First, the UMTS study is shown in Fig. 14 for the statistics calculated with the samples gathered at each position of the three corridor lines followed in the campaign. The standard deviation $\sigma_{\mathrm{Prx}}^{\mathrm{static}}(x,y)$ (blue circles) of the measurements for most points are lower than 2 dB, and its average is lower than 1 dB along the corridor (blue line). That indicates a very strong stability of most received power measurements for each position as a consequence of the average process performed by the app, which mitigates the fast-fading component of the propagation. Measurements in those positions with high standard deviation might suffer from the effect of cell-reselection due to shadowing. At the same time, the variation of the mean received power (green dots) at each position is also shown in Fig. 14, providing an assessment of the possibilities for discrimination of the different positions along the corridor.

Second, for GSM mobile telecommunications technology, Fig. 15 also shows high stability in each position of the corridor of the three lines, being $\sigma_{\mathrm{Prx}}^{\mathrm{static}}(x,y) = 0$ dB except for some few positions in each line where its value is increased, sometimes up to 10 dB. Once the serving cell was analyzed in each position, it was observed that these

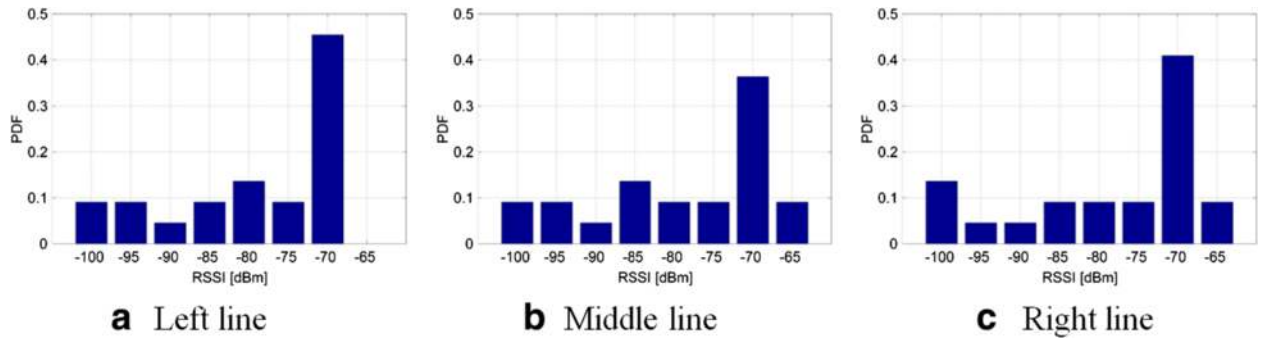

Fig. 11 GSM—Histograms (simulations) for the left (**a**), middle (**b**) and right (**c**) lines

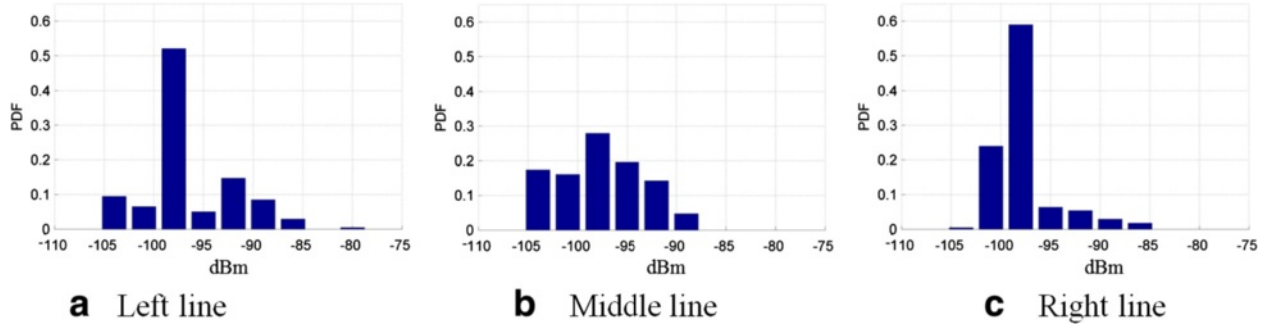

Fig. 12 UMTS—Histograms for the left (**a**), middle (**b**) and right (**c**) lines

big variations in the received power were caused by the cell-reselection mechanism. However, such behavior could easily be filtered based on the serving CellID information, providing still valuable information for those positions.

On the other hand, from the point of view of the serving CellID, these are depicted in Fig. 16a, where different icons identify each serving cell per position and line along the corridor. It is shown how UMTS terminals are connected to a wide variety of cells in this scenario, which explains the variations in the signal received in one spot. Conversely, as Fig. 16b depicts, the GSM signal presents homogeneous serving CellIDs in the corridor, except in the right side where the influence of several cells is presented. Such behaviors become convenient for localization purposes as it discriminates positions on the corridor.

In conclusion, both cellular technologies have shown a very strong stability in terms of the received power at the same position, especially if the consistency in the serving CellID is taken into account, while at the same time, it changes considerably along the corridor.

6.3 Applicability of the results

The analyzed characteristics of the analyzed technologies are now summarized. Table 1 shows the statistics for the signal complete distribution along the middle line of the corridor, while Table 2 shows the mean and median of the characteristics of variability obtained per position of the middle line.

For the case of RFID technology, the results on Prx corresponds to a tag placed on coordinates (0,1). In terms of Prx variability per adjacent position, it is observed how $\sigma_{\mathrm{Prx}}^{\mathrm{adjacent}}$ values are consistently high (median $\sigma_{\mathrm{Prx}}^{\mathrm{adjacent}} = 3.2$ dB), which makes it a good variable as input for the localization phase.

However, the signal presents a certain degree of instability per position (median$\sigma_{\mathrm{Prx}}^{\mathrm{static}} = 0.5$ dB), which may introduce inaccuracies during the real time localization phase. From the point of view of IDSrx, it is also observed that almost all tags are read in any position in the corridor. Therefore, the tag ID is not good enough to discriminate the real localization. As a consequence, each position is defined by the set of 30 RSSI fingerprints (each tag provides one).

In terms of cellular technology, on one hand, the low values in $\sigma_{\mathrm{Prx}}^{\mathrm{static}}(x,y)$ (median ≤ 0.2 dB for both cellular technologies) indicate a very strong stability in the measured signal for each point, which is a positive feature for localization purposes allowing a stable support for the positioning calculations. On the other hand, the high values in $\sigma_{\mathrm{Prx}}^{\mathrm{adjacent}}(x,y)$ provide an idea of the capability of distinguishing between different spots based on the cellular received power. Here, GSM, especially high

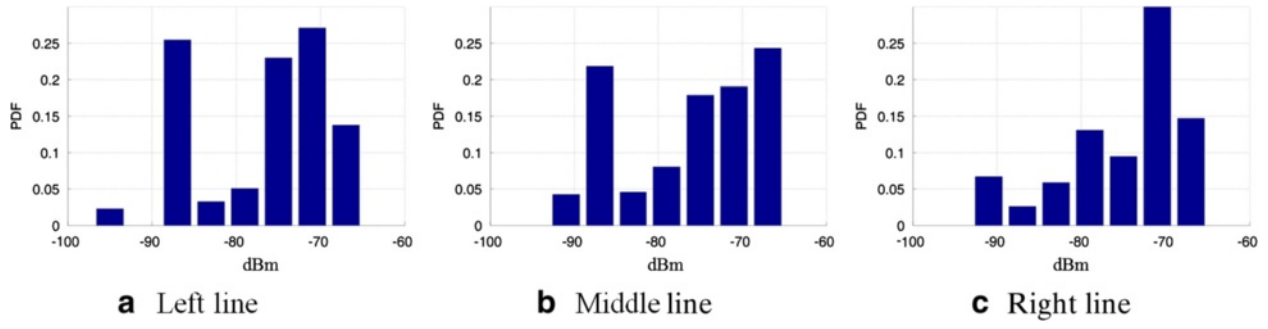

Fig. 13 GSM—Histograms for the left (**a**), middle (**b**) and right (**c**) lines

Fig. 14 UMTS—Received signal code power (RSCP) for the left (**a**), middle (**b**) and right (**c**) lines

values, indicate a strong advantage for the use of that signal in this purpose.

In terms of IDSrx, this means the variability of the received CellIDs, $N_{\mathrm{IDrs}}^{\mathrm{static}}(x,y)$ indicates that in general, more cells are received per position in UMTS, while $\sigma_{\mathrm{IDSrx}}^{\mathrm{adjacent}}(x,y)$ ratio represents the capability of distinguishing between adjacent positions based on the cell identifiers. Here, the latest indicates poor capabilities of GSM for the distinction based in cell id as most adjacent positions share the same cell id received $\left(\mathrm{median}\,\sigma_{\mathrm{IDSrx}}^{\mathrm{adjacent}}=0\right)$. Conversely, in the case of UMTS, each position is commonly a distinct pattern of receiving cells $\left(\mathrm{median}\,\sigma_{\mathrm{IDSrx}}^{\mathrm{adjacent}}=0.7\right)$ meaning that it is near one change of identifiers between positions).

It has to be indicated that these general conditions, as in any opportunistic system, may vary for different locations, as the distribution and composition of the macrocell environment may be different. So for the use of the macrocell information, an analysis of the particularities of each scenario has to be performed to assess the applicability of the scheme. In the analyzed scenario, the capabilities of position filtering based on UMTS IDSrx have shown the most promising qualities (instead of received signal), so it would be a key element for the enhancement achieved by the localization mechanism presented in the next section.

In any case, similar conditions have been reported in other analyzed scenarios, particularly in urban environment where, for example, the reception of multiple macrocells in each point is common. Also, the congruence with the simulated scenarios indicates the clear extrapolation of these characteristics.

7 Localization assessment

In this section, each localization system and their achieved synergies due to the integration of cellular

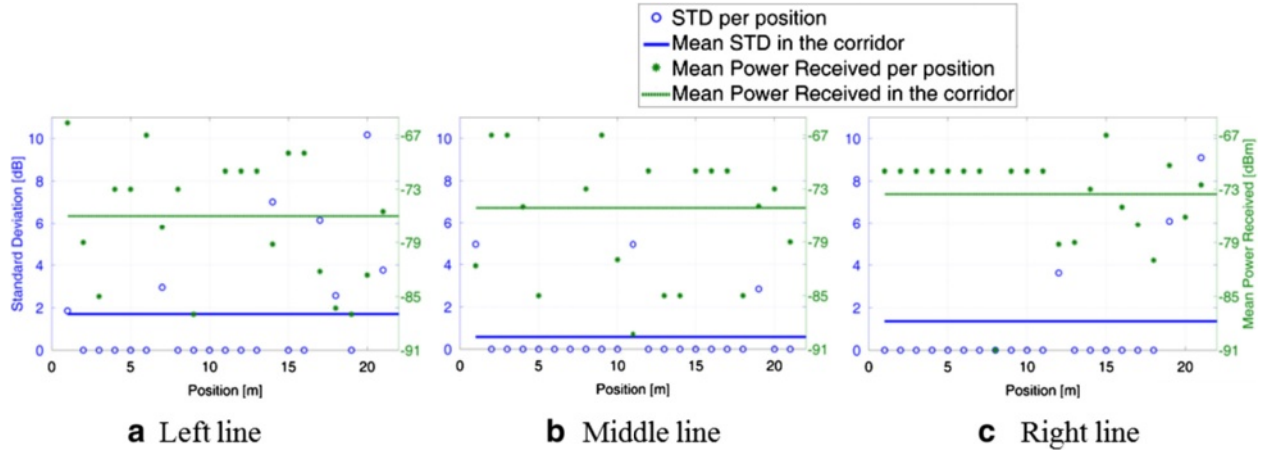

Fig. 15 GSM—Received signal level (RxLev) for the left (**a**), middle (**b**) and right (**c**) lines

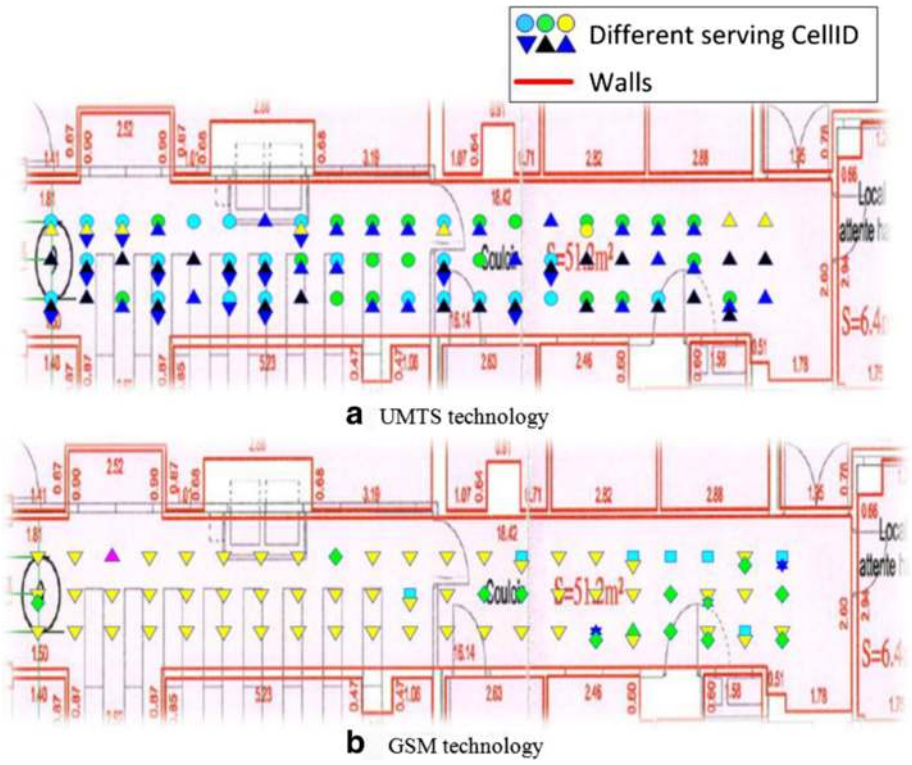

Fig. 16 UMTS and GSM—serving cell identifier for UMTS (**a**) and GSM (**b**) technologies

technologies in RFID-based localization systems are analyzed in the field of heterogeneous localization.

7.1 Localization RFID system

Fingerprinting has two main phases: *calibration* and *localization*. During the calibration phase, the RSSI values collected by the target (in this approach, the RFID reader) are measured at known locations and stored in a database. Concretely for this approach, the RSSI values are quantified with a resolution of 0.6 dBm as previously mentioned. Therefore, these quantified values are stored generating the electromagnetic "fingerprint" of the considered environment. During the localization phase, the target location is estimated by matching the new quantified RSSI values to those in the database. Different matching algorithms may be used to estimate the position.

7.1.1 Calibration phase

The calibration phase obtains the RFID fingerprint model. It consists on quantified RSSI measurements collected in a mesh of 30 × 30 cm as Fig. 17 shows. In the case under study, 75 acquisitions per line and 5 lines (375 fingerprinted positions) are included. The quantified data were recorded during 5 min at each point, which means 675,000 samples in the RFID system (60 samples per tag/position, 375 positions, and 30 tags) were saved. These measurements were gathered statically as the period of characterization was large, and it is the proper approach for the characterization of each point at calibration phase.

Table 1 Summary of signal variability (complete distribution)

Tech.	$\mu_{Prx}^{complete}$ (dBm)	$\sigma_{Prx}^{complete}$ (dB)	$N_{IDSrx}^{complete}$ (number)
RFID	−58.2	7.3	30
UMTS	−97.1	4.1	7
GSM	−75.1	7.5	4

7.1.2 Localization phase

After the calibration phase, the set of measurements received in real time by the localized platform was used to test the localization system. The measurements were dynamically performed in the middle row of the corridor

Table 2 Summary of signal variability (statistics per position middle line)

Tech.	Statistic	σ_{Prx}^{static} (dB)	$\sigma_{Prx}^{adjacent}$ (dB)	N_{IDSrx}^{static} (number)	$\sigma_{IDSrx}^{adjacent}$ (ratio)
RFID	Mean	0.7	3.2	28.7	1.4
	Median	0.5	3.2	29	1.0
UMTS	Mean	0.5	2.6	1.7	0.7
	Median	0.2	2.5	1.0	0.7
GSM	Mean	0.6	6.0	1.1	0.3
	Median	0.0	6.6	1.0	0.0

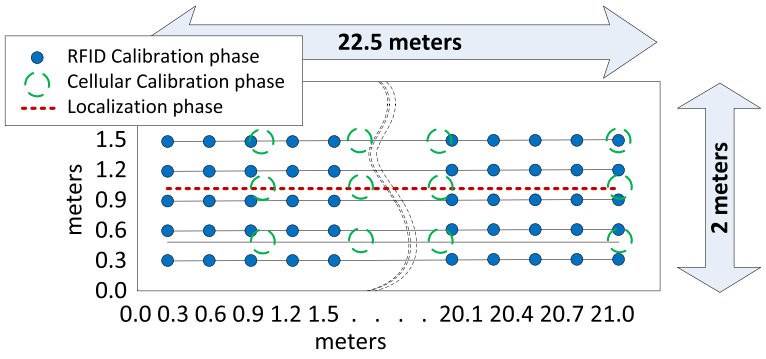

Fig. 17 Measured points

(red dotted line in Fig. 17), emulating the use of the system as an online localization platform. In this context, the acquisition time at each point is estimated in 5 s while the system takes a mean time less than 0.1 s to calculate the estimated position.

7.1.3 Results

The evaluation of this system is carried out in the middle line of the corridor by moving the mobile reader along it. The error between the real position and the computed positions are calculated for all the methods and combinations. Figure 18 shows the cumulative probability of the error distances for the presented methods. Figure 18a selects the candidates by the "number of matches" method, i.e., equal values in the quantified RSSI levels of the fingerprinting and the measurement positions. The four methods present similar characteristics, 95th percentile is around 4–5 m. Figure 18b also applies the "number of matches" method; however, in this case, the matches could be in the range of ±1 level compared with the calibration point. In this situation, the system reaches close to 3-m error distance in 95th percentile when the computed positions are calculated based on "kic" (k = 5) (red and green lines). In case the "mic" (maximum intersected candidates) method is selected, the error distance is increased. As observed, there

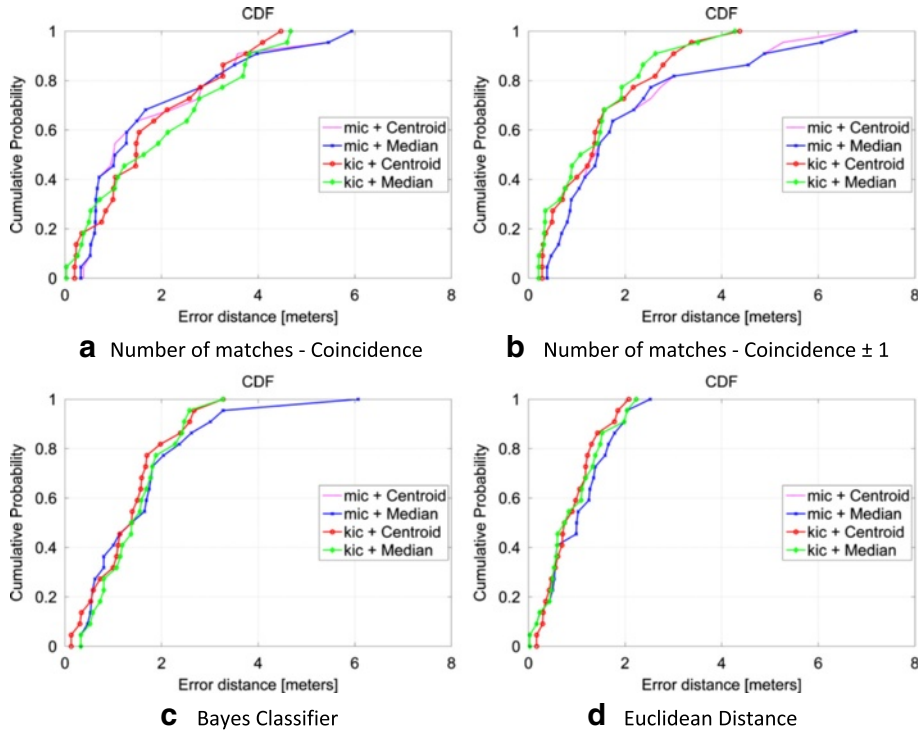

Fig. 18 RFID—Localization performance for the methods "number of matches – coincidence" (**a**), "number of matches – coincidence ±1" (**b**), "Bayes classifier" (**c**) and "Euclidean distance" (d)

is no significant difference between the centroid and the median metrics.

Similar behavior is observed in Fig. 18c for the "Bayes Classifier" method. In case the "mic" approach is selected, the 95th percentile is around 3 m while this error is enhanced by the "kic" approach. In this case, the 95th percentile is below 2.5 m.

In Fig. 18d, the results of the "Euclidean distance" method are depicted. Clearly, this method shows the best performance compared to the others. It could reduce the 95th percentile to 2 m. That error is enhanced when the positions are estimated based on the "kic" (k = 5).

7.2 Localization cellular system

7.2.1 Calibration phase

For the cellular model, the measurements are recorded along the corridor every meter following 3 lines on the floor with a distance of 50 cm from each other (63 positions) as Fig. 17 shows. In this case, as the "Signal assessment" section has concluded, the selected parameter to complete the calibration phase is the CellID, i.e., the cell identifier. Therefore, CellID information was recorded during 5 min at each point, which implies that around 37,800 samples in the whole scenario from the cellular system (18,900 samples per technology GSM or UMTS) were stored.

7.2.2 Localization phase

The localization phase was carried out at the same time as RFID localization phase; therefore, it followed the same period as RFID system to collect measurements (5 s) and similar time to calculate the estimated position (less than 0.1 s).

7.2.3 Results

The evaluation of the cellular technology-based positioning system is based on the measured CellIDs. Therefore, the accuracy is much lower than RFID-based systems. However, the density of base stations in the corridor could create clusters to then discriminate and enhance other localization system at indoor environments. Figure 19 shows the cumulative probability of this cellular system where, as expected, the error distance is quite high. The 95th percentile is around 10 m.

7.3 Opportunistic localization system

The period to calculate the estimated position was established in every 5 s; however, as the algorithms do not involve high computational costs, the position is estimated in an average time of 100 ms: 60 ms to get RFID candidates and 35 ms to get cellular candidates (parallel processes could reduce this time). Table 3 compares the results obtained with the RFID localization methods to be compared to the opportunistic localization technique (i.e., RFID and cellular combination). Due to the similar results, only centroid metric has been included in the table.

The cellular discrimination phase discards some candidates for all methods, excepting the "Euclidean distance" and "Bayes Classifier" methods (since the RFID phase only proposed one candidate in that case). On the one hand, for the RFID system, the mean absolute error is below 2 m and the 95th percentile is between 3.5 and 5.5 for the first two methods. On the other hand, the integration of cellular information into the discrimination procedure discards some candidates that could be far away from the real position. Thanks to it, the proposed system is able to reduce the mean absolute

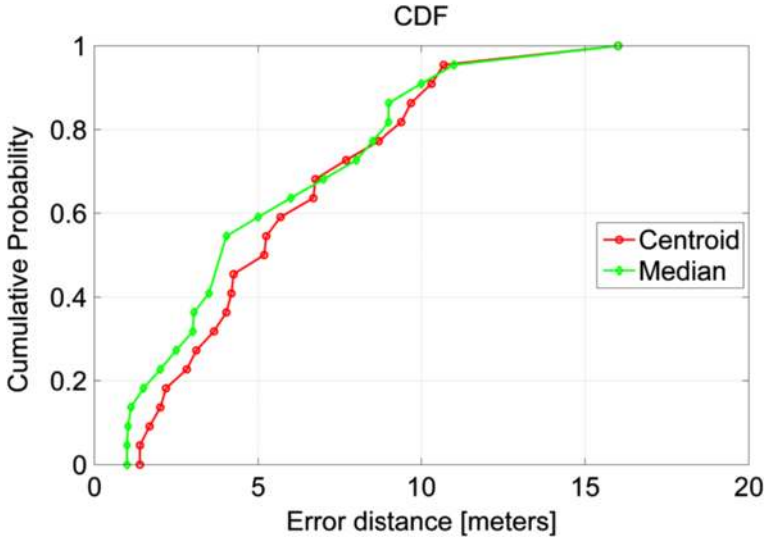

Fig. 19 Cellular—Localization performance

Table 3 Summary of localization

	Same level		±1 level		Probabilistic		Euclidean distance	
	mic	kic	mic	kic	mic	kic	mic	kic
RFID system mean absolute error (m)	1.9	1.8	2.1	1.3	1.6	1.3	1.1	0.9
RFID System MSE	6.7	5.9	7.4	4.5	5.6	3.9	3.6	3.1
RFID System 95th percentile	5.5	4.1	5.3	3.5	3.4	2.6	2.0	1.9
Integrated system mean absolute error (m)	1.5	1.4	1.8	1.1	1.6	1.2	1.1	0.9
Integrated system MSE	5.5	4.0	5.8	3.7	5.6	3.7	3.6	3.0
Integrated system 95th percentile	3.2	3	3.7	2.2	3.4	2.5	2.0	1.8

error from 15 to 25 % in comparison to the RFID-based localization system. This enhancement provides mean absolute error values from 1.1 to 1.8 m. In the same context, the 95th percentile is reduced for most methods, reaching values from 2 to 3.7 m. The "Bayes Classifier" and "Euclidean distance" methods are slightly improved when more than one candidate is selected ("kic" approach).

For the best method (Euclidean distance, kic), results show 1.4 m for the 80th percentile and 1.8 m for the 95th percentile. Compared with the state of the art, 1.5-m mean absolute error is obtained in [1], and 1 m at 80th percentile, but 4 m at 90th percentile, are obtained in [16]. Furthermore, in reference [6], the RFID system is quite similar in terms of hardware (a mesh of 19 RFID sensors and 19 active RFID reference tags) while this work uses 30 active tags for similar performances. The 95 % cumulative percentile of error distance is approximately 3 m in [6] but 1.8 m in this study. Actually, within indoor environments, the corridor is the most critical. In references [27] and [28], the cumulative distribution function (CDF) is compared for RSS-based localization techniques in different environments, big and small rooms, research laboratory, and corridors. It is clear from these studies that accuracy becomes twice as bad in corridors than in large rooms or labs. Moreover, using the already deployed technologies such as cellular technologies allow us to reduce the signal processing complexity for a real time localization.

Therefore, this approach for the combination of both technologies increases the localization accuracy and precision. It reflects the potentialities of their integration for indoor localization.

7.4 Sensitivity study

A sensitivity study has been performed to evaluate this approach in the same scenario with a low-dense number of tags. The number of tags has been reduced according to 1/2, 1/3, and 1/5 from the original amount (30 tags). Tables 4 and 5 present the mean square error (MSE) of the RFID system and the proposed system, respectively. It could be observed in both tables how the less number of tags are placed; the worse MSE values are obtained. Furthermore, with high dense of tags, cellular technology improve the location accuracy over the RFID system. However, when the number of tags is extremely reduced, the influence of cellular technology does not enhance the location error as much as expected. The reason is related with the low number of candidates the RFID system proposes; therefore, the discrimination of cellular technology is much more limited to those candidates.

7.5 Considerations for real deployments

By the time of this work, cost of each active tag is in the range of tens of United States dollars (USDs) while a RFID reader rounds few hundred USDs costs. Therefore, the defined RFID system is based on the distribution of RFID tags in the infrastructure, while the localized platform (e.g., pedestrian equipment) to be positioned is provided with a RFID tag reader, which is the optimal solution if a reasonable amount of mobile equipments are to be localized in a wide and complex area. In this way, the infrastructure costs are minimized while placing the cost in the positioned object. This greatly reduces installation costs and allows the implementation of the system in large areas at minimum expense. Additionally, the commercial penetration of portable RFID readers is

Table 4 Sensitivity study of RFID system based on the number of tags (MSE)

RFID system MSE	Same level		±1 level		Probabilistic		Euclidean distance	
	mic	kic	mic	kic	mic	kic	mic	kic
30 tags (ratio 1)	6.7	5.9	7.4	4.5	5.6	3.9	3.6	3.1
15 tags (ratio 1/2)	15.6	9.9	9.1	6.5	9.2	6.0	5.6	4.8
10 tags (ratio 1/3)	24.4	20.8	14.3	11.0	13.5	10.9	9.8	8.7
6 tags (ratio 1/5)	43.8	38.9	31.7	21.2	26.7	19.6	16.9	14.6

Table 5 Sensitivity study based on the number of tags (MSE)

Integrated systemMSE	Same level		±1 level		Probabilistic		Euclidean distance	
	mic	kic	mic	kic	mic	kic	mic	kic
30 tags (ratio 1)	5.5	4.0	5.8	3.7	5.6	3.7	3.6	3.0
15 tags (ratio 1/2)	15.0	9.1	9.1	5.9	9.2	5.8	5.6	5.1
10 tags (ratio 1/3)	23.1	11.8	12.2	8.1	13.5	10.7	9.8	9.6
6 tags (ratio 1/5)	40.0	38.8	27.9	19.5	26.7	18.5	16.9	15.8

growing, being also included in mobile phones as peripherals or embedded systems [29]. In any case, scenarios where the located system is equipped with RFID tags instead of a transceiver (being the transceivers part of the fixed infrastructure of the scenario) are also possible [30, 31], keeping the same general scheme and conditions in terms of performance and architectural needs.

In order to cover an entire floor of a public building of some hundreds square meters with passive tags, a few hundreds of readers must be deployed, as their read range is 1–3 m. Using active tags allows to cover a whole floor, without increasing the total number of tags. Further studies on the optimal number of tags and their placement are being carried out for the corridor [32] and the entire floor. Therefore, active RFID solution is still cost effective when covering large areas even if we locate a hundred of mobile readers.

In the proposed approach, the main elements of classical architectures for RFID-based localization are maintained: a remote localization server performs the calculation of the position based on the signals received from the RFID tags and the previously stored fingerprint data. The only additions to this classic structure imply the inclusion of cellular signal fingerprint information as part of the localization server databases and the existence of a cellular receiver as part of the localized platform. The cellular receiver may be already part of the localized platform (e.g., for communications reasons). Otherwise, adding the cellular receiver to the previously existing pure RFID platforms can be done at a very low cost due to the wide popularity of the cellular technology: a low-budget smartphone may be enough. Additionally, the increasing availability of RFID commercial portable readers for active RFID tags could make this approach even more accessible for pedestrian applications in the close future.

The acquisition of cellular technologies fingerprint data should also not suppose any significant cost in terms of the calibration phase, as the cellular scenario characterization can be performed simultaneously to the RFID one.

A shortcoming of the proposed system is that if the cellular infrastructure changes due to modifications done by operators (e.g., change of configuration parameters) or failure, the accuracy of the cellular-based discrimination can be jeopardized and a new fingerprint calibration phase may be required. This is the same case as for changes in the RFID infrastructure, but the latter is usually more accessible and under the control of local administrators. In order to overcome this challenge, coordination between the mobile operator and the localization system should be defined, fitting in the initiated process by cellular standardization aiming to integrate localization (including the one coming from third party solutions) as part of the standard architecture interfaces [33, 34].

Another issue arises when the indoor area is covered by only one (or few) base stations, which makes the cellular information useless or not be as helpful as expected. However, the experience has shown that most of the time, a certain level of signal is received from several cells simultaneously (it does not mean the quality of the signal is appropriate to attempt a call) or cellular technologies. Furthermore, the increasing deployments of small cells will help to further avoid this restriction.

To conclude, the use of common application layer apps for the mobile terminal is assumed as the source of signal information. However, one of the main limitations of some terminals (due to their manufacturers) is their inability to report information about neighbor cells (e.g., received power, CellID, etc.). That issue would affect the fingerprint procedure as it could suffer from lack of information. However, handover/cell-reselection process would be useful in order to overcome this lack of information from several cells. Regarding this issue, this study has taken into account that restriction, focusing on this kind of terminals (e.g., Samsung) as a high percentage of smartphones, has this limitation.

8 Conclusions

In this paper, the fundamentals for innovative RFID localization systems with opportunistic use of GSM and UMTS measurements have been presented. Here, the analysis assesses the possibilities of using signals coming from already existent non-positioning-oriented cellular networks to provide support to indoor RFID-based positioning mechanisms, which could highly benefit from such pre-existent communication infrastructure. Furthermore,

the use of a first-approach, fingerprinting mechanism for localization shows promising results in terms of accuracy enhancement.

Results show a mean absolute error around 1 m, while the 95th percentile is 2 m.

Abbreviations

AoA: Angle of Arrival; CDF: Cumulative Distribution Function; CERP: Cooperative Eigen-Radio Positioning; DMRF: Direct Multi-Radio Fusion; DVB: Digital Video Broadcasting; FM: Frequency Modulation; GSM: Global System for Mobile Communications; HetNets: Heterogeneous Networks; LAC: Local Area Code; LBS: Location-Based Services; LoS: Line of Sight; MSE: Mean Square Error; OFDM: Orthogonal Frequency Division Multiplexing; PDF: Probability Density Function; RF: RadioFrequency; RFID: Radio-Frequency IDentification; RSSI: Received Signal Strength Indicator; RTD: Round-Trip Delay; ToF: Time of Flight; UMTS: Universal Mobile Telecommunications System; USD: United States Dollars; UWB: Ultra Wide Band; WLAN: Wireless Local Area Network.

Competing interests

The authors declare that they have no competing interests.

Acknowledgements

This work has been partially funded by Junta de Andalucía (Proyecto de Investigación de Excelencia P12-TIC-2905). We deeply thank Marc Hayoz for endless hours of measurements.

Author details

[1]Departamento de Ingeniería de Comunicaciones, Universidad de Málaga, Andalucía Tech, Campus de Teatinos s/n, 29071 Málaga, Spain. [2]ESIGETEL, Allianstic, Villejuif, France.

Received: 1 November 2014 Accepted: 8 September 2015
Published online: 28 September 2015

References

1. AM Vegni, F Esposito, "Location aware mobility assisted services for heterogeneous wireless technologies", Wireless Sensing, Local Positioning, and RFID. IEEE MTT-S International Microwave Workshop, vol., no., pp.1,4, 24–25 September. 2009
2. R Mautz, *"Indoor positioning technologies"* (Habilitation Thesis, ETH Zurich, 2012), p. 127
3. N Pathanawongthum, P Cherntanomwong, "RFID based localization techniques for indoor environment." In Advanced Communication Technology (ICACT), 2010 The 12th International Conference on (Vol. 2, pp. 1418–1421). IEEE. February 2010.
4. K Chawla, G Robins, L Zhang, "Object localization using RFID." In Wireless Pervasive Computing (ISWPC), 2010 5th IEEE International Symposium on (pp. 301–306). IEEE. May 2010.
5. SL Ting, SK Kwok, AH Tsang, GT Ho, "The study on using passive RFID tags for indoor positioning". Int. J. Eng. Bus. Manage. **3**(1), 9–15 (2010)
6. Z Han, W Hengtao, X Lihua, J Qing-Shan, "An RFID indoor positioning system by using weighted path loss and extreme learning machine," Cyber-Physical Systems, Networks, and Applications (CPSNA), 2013 IEEE 1st International Conference on, vol., no., pp.66,71, 19–20 Aug. 2013
7. R Mautz, *"Indoor positioning technologies" (Doctoral dissertation, Habil. ETH Zürich, 2012)* (Venia Legendi in Positioning and Engineering Geodesy Institute of Geodesy and Photogrammetry, Department of Civil, Environmental and Geomatic Engineering, ETH Zurich, 2012)
8. "Small cells—what's the big idea. Femtocells are expanding beyond the home," white paper, Small Cell Forum Ltd, Februery. 2012
9. M Molina-García, J Calle-Sánchez, JI Alonso, A Fernández-Durán, FB Barba, "Enhanced in-building fingerprint positioning using femtocell networks". Bell Labs Tech. J. **18**, 195–211 (2013). doi:10.1002/bltj.21613
10. FB Barba, AG Martin, A Fernández-Durán, "Wireless indoor positioning: effective deployment of cells and auto-calibration". Bell Labs Tech. J. **18**, 213–235 (2013). doi:10.1002/bltj.21614
11. S Sand, C Mensing, Y Ma, R Tafazolli, X Yin, J Figueiras, J Nielsen, BH Fleury, "Hybrid data fusion and cooperative schemes for wireless positioning," Vehicular Technology Conference, 2008. VTC 2008-Fall. IEEE 68th, vol., no., pp.1,5, 21–24 September 2008
12. S-H Fang, T-N Lin, Cooperative multi-radio localization in heterogeneous wireless networks. Wireless Communications, IEEE Transactions **9**(5), 1547–1551 (2010)
13. A Papapostolou, H Chaouchi, "Simulation-based analysis for a heterogeneous indoor localization scheme," Consumer Communications and Networking Conference (CCNC), 2010 7th IEEE, vol., no., pp.1,5, 9–12 January. 2010
14. L Xingchuan, M Qingshan, L Henghui, L Xiaokang, "Wi-Fi/MARG/GPS integrated system for seamless mobile positioning," Wireless Communications and Networking Conference (WCNC), 2013 IEEE, vol., no., pp.2323,2328, 7–10 April 2013
15. S Zhang, W Xiao, B Zhang, BH Soong, "Wireless indoor localization for heterogeneous mobile devices," Computational Problem-Solving (ICCP), 2012 International Conference on, vol., no., pp.96,100, 19–21 October. 2012
16. B Denis, R Raulefs, BH Fleury, B Uguen, N Amiot, L de Celis, J Dominguez, MB Koldsgaard, M Laaraiedh, H Noureddine, E Staudinger, G Steinboeck, "Cooperative and heterogeneous indoor localization experiments," Communications Workshops (ICC), 2013 IEEE International Conference on, vol., no., pp.6,10, 9–13 June 2013
17. PV Nikitin, KVS Rao, "Performance limitations of passive UHF RFID systems," Antennas and Propagation Society International Symposium 2006, IEEE, vol., no., pp.1011,1014, 9–14 July 2006
18. SY Seidel, TS Rappaport, 914 MHz path loss prediction models for indoor wireless communications in multifloored buildings. Antennas and Propagation, IEEE Transactions **40**(2), 207–217 (1992)
19. European Cooperation in the Field of Scientific and Technical Research, EURO-COST 231, "Digital mobile radio towards future generation systems", COST 231 Final report. [Online] http://www.lx.it.pt/cost231/
20. WINNER II IST project, "D1.1.2. WINNER II channel models. part II. radio channel measurement and analysis results. v1.0," WINNER II IST project, Tech. Rep., 2007. [Online]. Available: www.ist-winner.org/. Accessed October 2014
21. H Liu, H Darabi, P Banerjee, J Liu, "Survey of wireless indoor positioning techniques and systems". IEEE Trans Syst Man Cybern C Appl. Rev. **37**(6), 1067–1080 (2007)
22. Christopher D. Manning, Prabhakar Raghavan, and Hinrich Schütze. Introduction to Information Retrieval. New York, NY, USA: Cambridge University Press; 2008.
23. LM Ni, Y Liu, YC Lau, AP Patil. LANDMARC: indoor location sensing using active RFID. Wirel. Netw. **10**(6), 701–710 (2004). doi:10.1023/B:WINE.0000044029.06344.dd
24. Ela Innovation SA, Ela Innovation active RFID tag and reader manufacturer. http://www.rfid-ela.eu/. Accessed October 2014
25. G-MoN Application. [Online]. Available: https://www.wardriving-forum.de/wiki/G-MoN. Accessed October 2014
26. 3GPP Technical Specification 36.331, "Evolved Universal Terrestrial Radio Access (E-UTRA); Radio Resource Control (RRC); Protocol Specification (Release 8)", December 2008
27. K Wu, J Xiao, Y Yi, M Gao, LM Ni, "FILA: Fine-grained indoor localization," INFOCOM, 2012 Proceedings IEEE, vol., no., pp.2210,2218, 25–30 March 2012
28. Y Chen, N Crespi, L Lv, M Li, AM Ortiz, L Shu, "Locating using prior information: wireless indoor localization algorithm." In ACM SIGCOMM Computer Communication Review (Vol. 43, No. 4, pp. 463–464). ACM, August, 2013
29. J-B Eom, S-B Yim, T-J Lee, "An efficient reader anticollision algorithm in dense RFID networks with mobile RFID readers," Industrial Electronics, IEEE Transactions on, vol.56, no.7, pp.2326,2336, July 2009
30. S Chatrati, S Naidu, CR Prasad, "RFID based student monitoring and attendance tracking system," Computing, Communications and Networking Technologies (ICCCNT),2013 Fourth International Conference on, vol., no., pp.1,5, 4–6 July 2013
31. J Maneesilp, W Chong, W Hongyi, T Nian-Feng, "RFID support for accurate 3D localization". Computers, IEEE Transactions **62**(7), 1447–1459 (2013)
32. V Oruganti, V Gharat, E Colin, A Moretto, "Location performance law according to the dimensions of the corridor using tri/multilateration"

Proceedings Fifth International Conference on Indoor Positioning and Indoor Navigation, IEEE GRSS, October 2014
33. 3GPP TS 23.271 V12.0.0 (2013–12) "3rd Generation Partnership Project; Technical Specification Group Services and System Aspects; Functional stage 2 description of Location Services (LCS) (Release 12)"
34. S Fortes, A Aguilar-García, R Barco, F Barba, JA Fernández-Luque, A Fernández-Durán, Management Architecture for Location-Aware Self-Organizing LTE/LTE-A Small Cell Networks. IEEE Communications Magazine, January 2015